Electronic Supplementary Information for:

Time-Resolved Transient Optical and Electron Paramagnetic Resonance Spectroscopic Studies of Electron Donor-Acceptor Thermally Activated Delayed Fluorescence Emitters Based on Naphthalimide-Phenothiazine Dyads

Kaiyue Ye,‡[a] Andrey A. Sukhanov,‡[b] Yu Pang,‡[c] Aidar Mambetov,[b] Minjie Li,[d] Liyuan Cao,[a] Jianzhang Zhao,*[a] Violeta K. Voronkova,*[b] Qian Peng*[c] and Yan Wan*[d]

[a] State Key Laboratory of Fine Chemicals, Frontiers Science Center for Smart Materials, School of Chemical Engineering, Dalian University of Technology, Dalian 116024, P. R. China. * E-mail: zhaojzh@dlut.edu.cn (J. Z.)

[b] Zavoisky Physical-Technical Institute, FRC Kazan Scientific Center of Russian Academy of Sciences, Kazan 420029, Russia. * E-mail: vor18@yandex.ru (V. K. V.)

[c] School of Chemical Sciences, University of Chinese Academy of Sciences, Beijing 100049, P. R. China. * E-mail: qianpeng@ucas.ac.cn (Q. P.)

[d] College of Chemistry Beijing Normal University, Beijing 100875, P. R. China. * E-mail: wanyan@bnu.edu.cn (Y. W.)

‡ K. Y., A. A. S. and Y. P. contributed equally to this work.

Table of Contents

1. Experimental section

Femtosecond Transient Absorption Spectra.

Femtosecond transient absorption spectra (fs-TA) were acquired on a system based on a Ti:sapphire regenerative amplifier (Amplitude Pulsar) pumped by a homemade Ti:sapphire oscillator. The system produces 40 fs pulses at 800 nm, with a repetition rate of 1 kHz and average power of 450–500 mW. The instrument resolution is 150 fs. Excitation pulses at 340 nm were produced by third harmonic generation from the output of a commercial parametric amplifier (TOPAS, Light Conversion) using two BBO crystals. The pump beam polarization has been set to the magic angle with respect to the probe beam. The probe beam has been obtained by focusing a small portion of the fundamental 800 nm beam on a 3 mm CaF_2 crystal, kept under continuous rotation to avoid damage. The pump-probe delay has been introduced by sending the portion of the fundamental beam used for white light generation through a motorized translator. After focusing and overlapping the pump and probe beams at the sample position, the probe beam has been directed through a spectrograph and to the detector. The sample was contained in a 2 mm quartz cuvette mounted on a movable stage, in order to avoid photo-decomposition. The data were subdivided in two different time intervals and fitted using the Glotaran-Application 1.5.1 software.[1] The number of kinetic components to be used for Global analysis has been estimated by performing a preliminary singular values decomposition (SVD) analysis. All data were chirp-corrected before global fitting.

Time-Resolved Electron Paramagnetic Resonance (TREPR) Spectroscopy.

Samples were dissolved in frozen toluene/2-me-tetrahydrofuran (TOL/2MeTHF) solvent. The time-resolved continuous-wave (CW) TREPR measurements were performed on an X-band EPR Elexsys E−580 spectrometer (Bruker). TREPR spectra was recorded at 20 K, 40 K and 80 K in TOL/2MeTHF mixed solutions, and 80 K and 140 K in TOL. Optical excitation was carried out with an optical parametric oscillator (OPO) system (LP603 SolarLS) pumped by an Nd:YAG laser (LQ629 SolarLS) with a pulse energy of 1 mJ. The numerical simulations of the TREPR spectra were performed using a modified version of a program described in detail previously.[2,3] The spectrum integrated over a chosen time interval is calculated for a quasi-random distribution of fixed orientations of the compounds relative to the laboratory frame in the linear response approximation. The fitting is based on the least-squares method. The values of the adjustable parameters were

obtained by a simultaneous fit of several experimental spectra extracted from the time/magnetic field data set in time intervals chosen to represent critical regions of the time dependence.

Computational method. The molecular geometries of **NI-PTZ** in the S_0 state are optimized at CAM-B3LYP/6-31G(d) level, solvent effects were included using the polarizable continuum model (PCM), the excited states geometries of S_1 and T_1 are optimized with time-dependent DFT (TD-DFT) in its Tamm-Dancoff approximation (TDA) using the same functional and basis sets as in the ground-state optimizations, all calculations are performed using the Gaussian 16 program package.[4] The spin-orbit matrix elements (SOCME) are calculated, as implemented in Q-chem software.[5] The Zero-Field Splitting (ZFS) parameters D are calculated using B3LYP/def2-TZVP method with TD-DFT in Orca software.[6,7]

2. Steady state UV–vis absorption and luminescence spectra
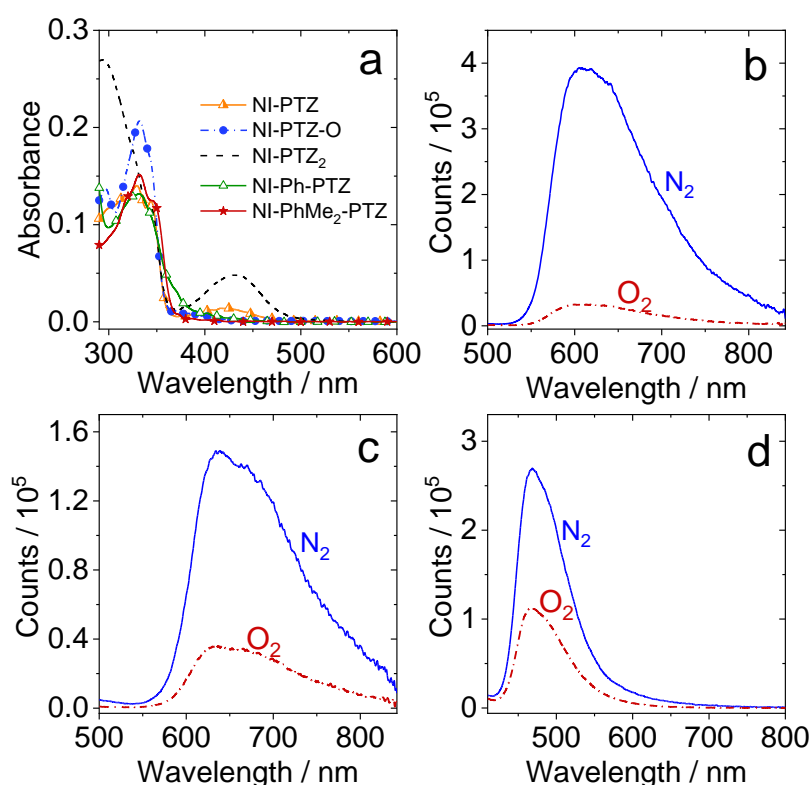
Figure S1. (a) UV–vis absorption spectra of **NI-PTZ**; **NI-PTZ-O**; **NI-PTZ₂**; **NI-Ph-PTZ** and **NI-PhMe₂-PTZ** in acetonitrile (ACN). $c = 1.0 \times 10^{-5}$ M. Fluorescence spectra of the compounds of (b) **NI-PTZ**, (c) **NI-PTZ₂** and (d) **NI-PTZ-O** in HEX under different atmospheres (N₂, O₂). Optically-matched solutions were used, A = 0.10, λ_{ex} = 330 nm, $c = 1.0 \times 10^{-5}$ M, 20 °C.

3. Femtosecond transient absorption spectra
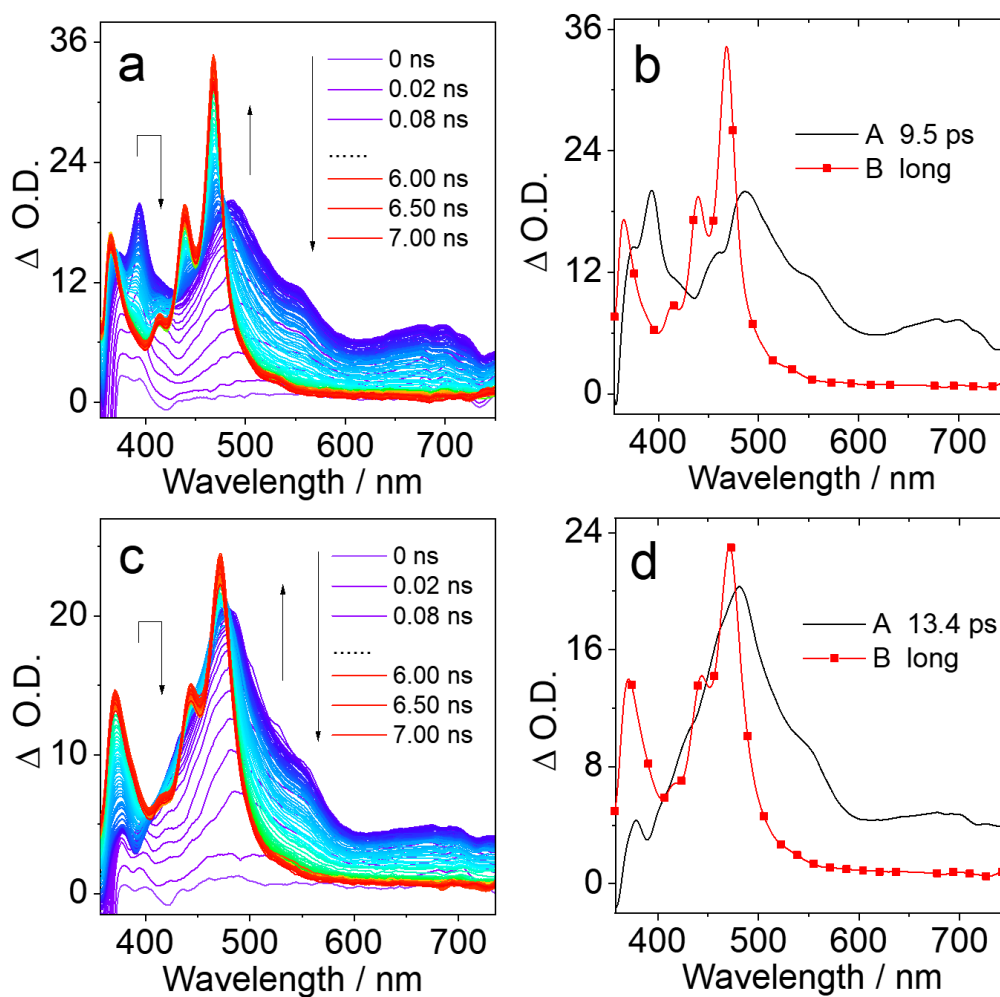
Figure S2. Femtosecond transient absorption spectra of **NI-3Br**. Transient absorption spectra (a) in HEX and (c) in ACN. Relative EADS obtained with global analysis (b) in HEX and (d) in ACN. Excited at 330 nm.

NI-3Br
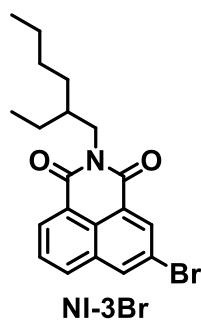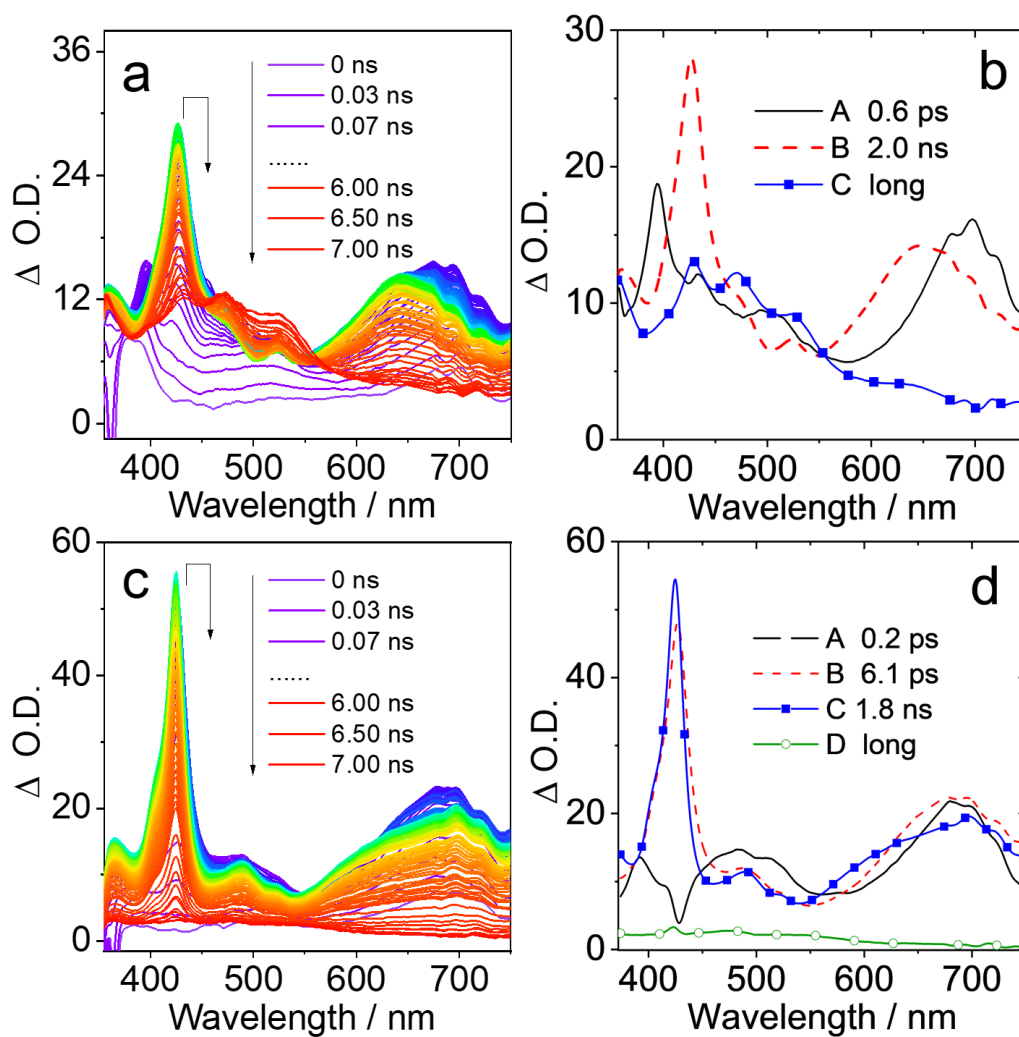
Figure S3. Femtosecond transient absorption spectra of **NI-PTZ-O**. Transient absorption spectra (a) in HEX and (c) in ACN. Relative EADS obtained with global analysis (b) in HEX and (d) in ACN. Excited at 330 nm.
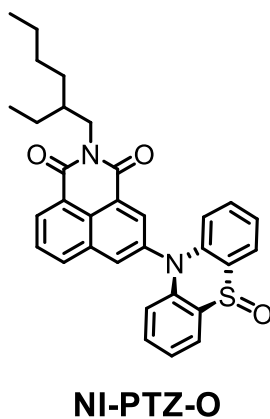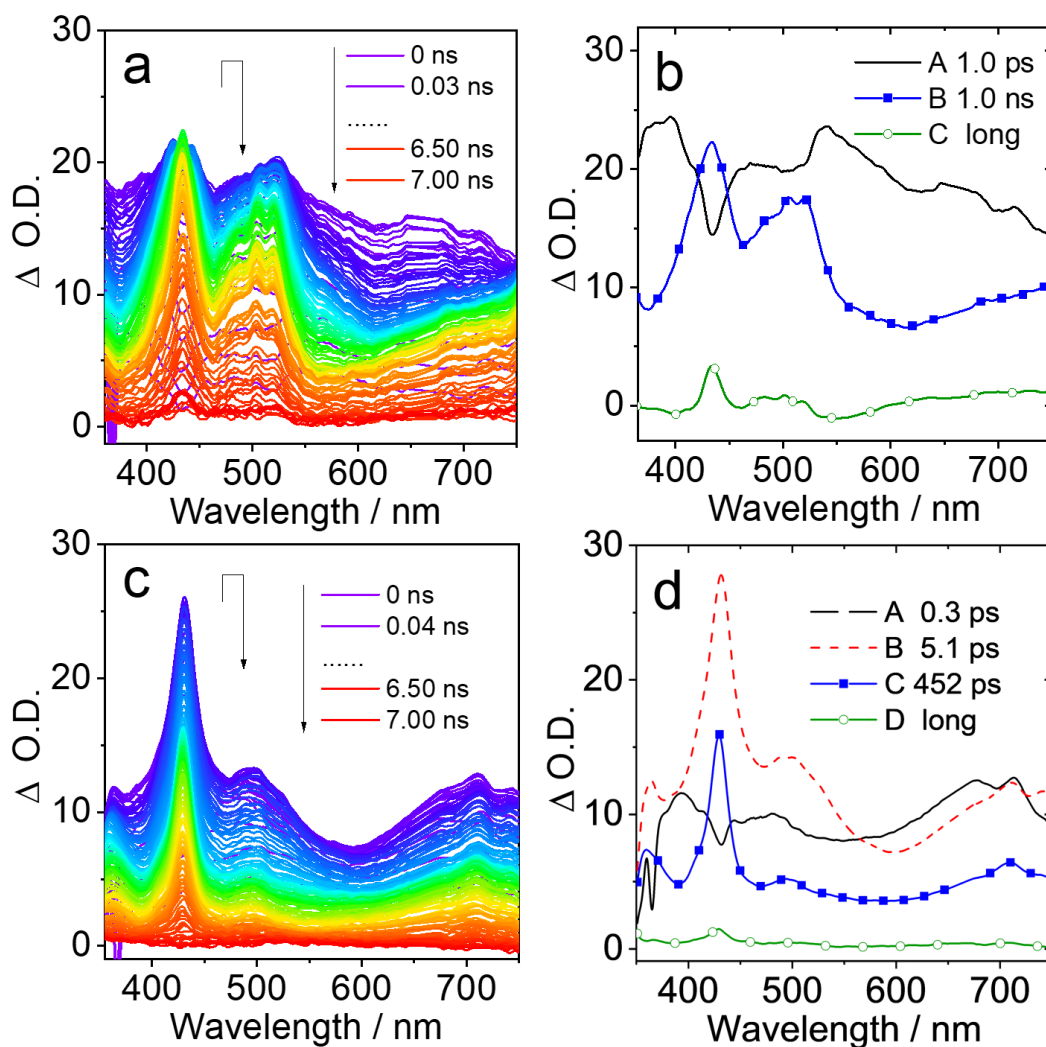
NI-PTZ-O

Figure S4. Femtosecond transient absorption spectra of **NI-PTZ₂**. Transient absorption spectra (a) in HEX and (c) in ACN. Relative EADS obtained with global analysis (b) in HEX and (d) in ACN. Excited at 330 nm.

NI-PTZ₂
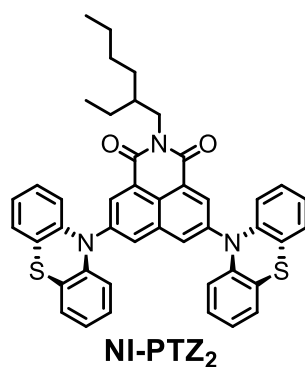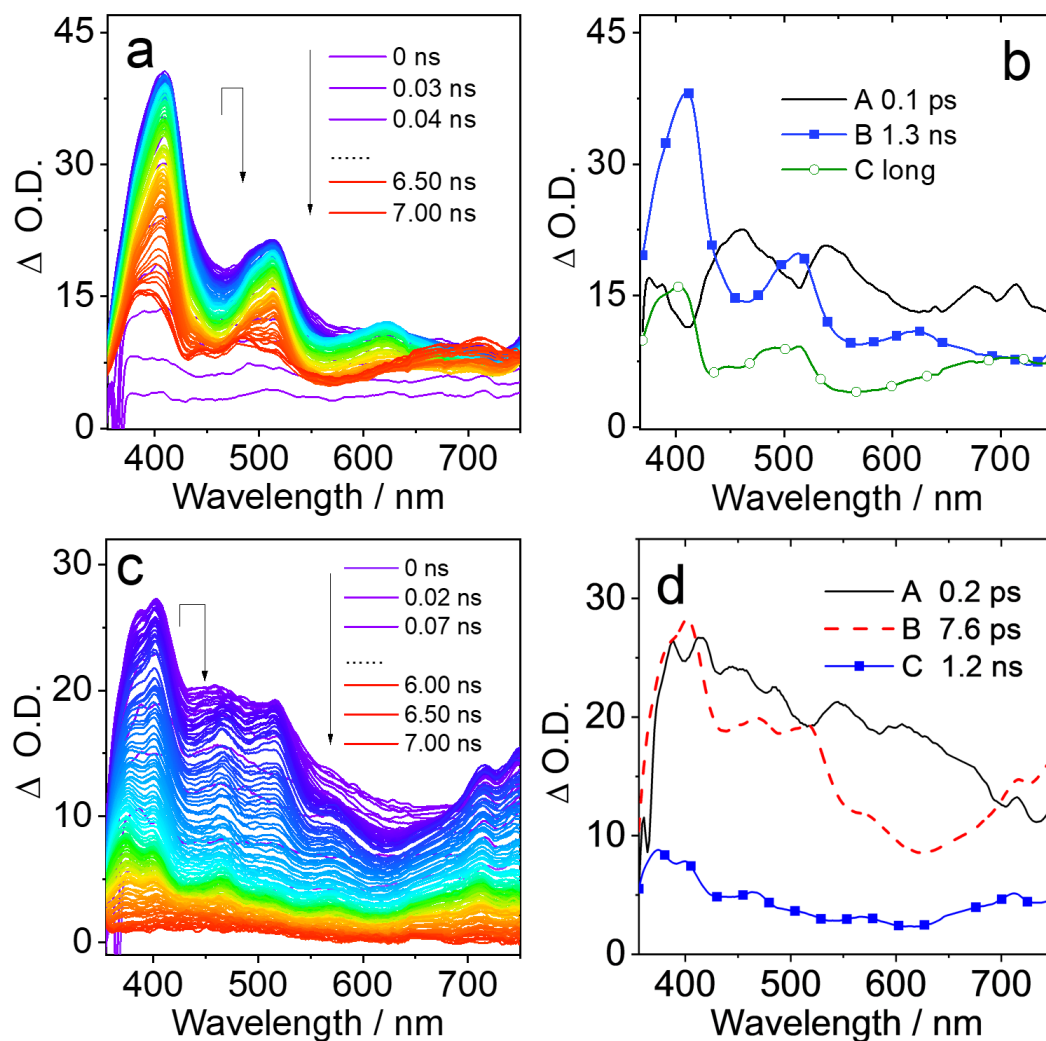
Figure S5. Femtosecond transient absorption spectra of **NI-Ph-PTZ**. Transient absorption spectra (a) in HEX and (c) in ACN. Relative EADS obtained with global analysis (b) in HEX and (d) in ACN. Excited at 330 nm.

NI-Ph-PTZ
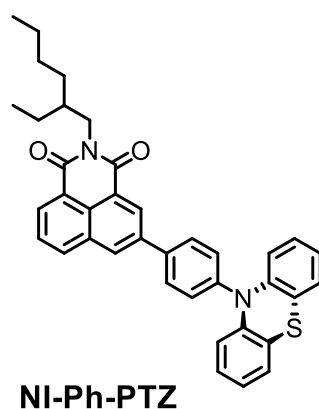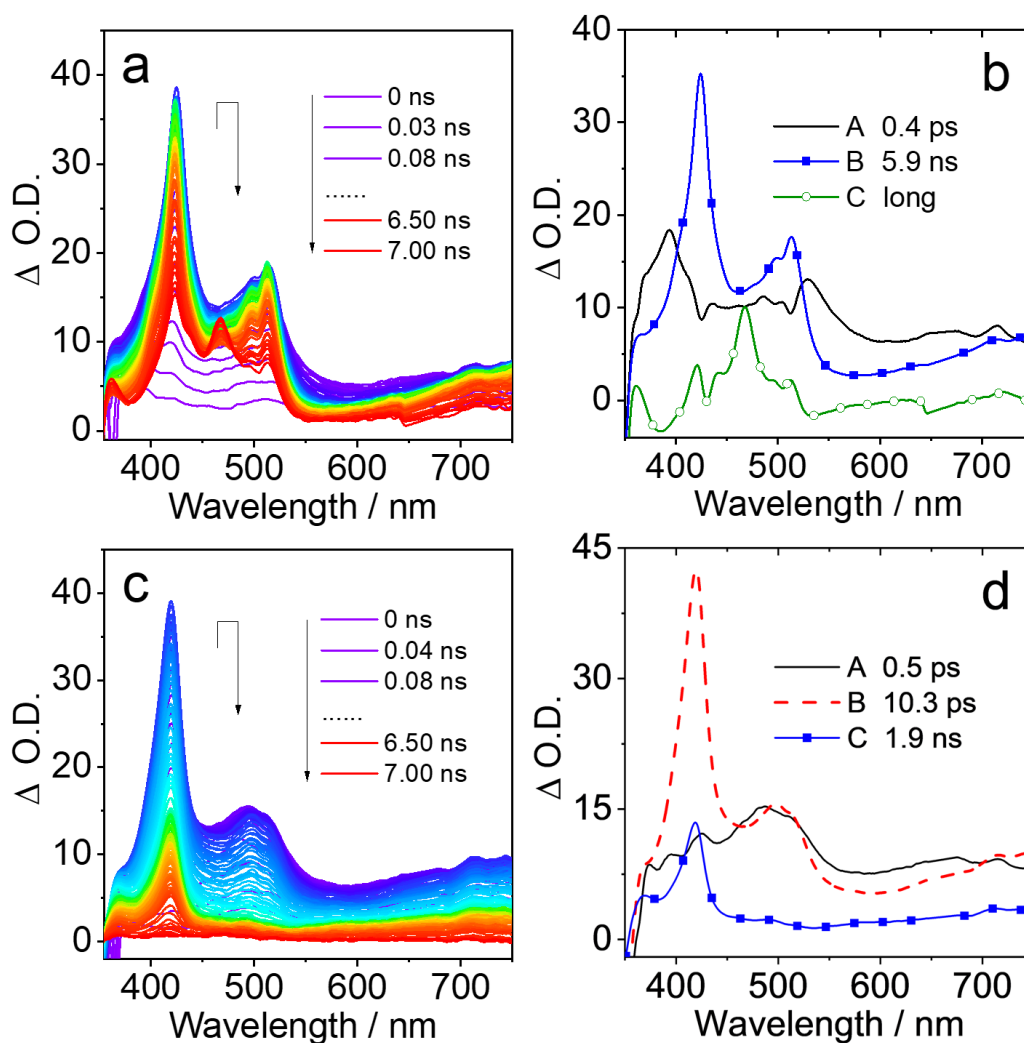
Figure S6. Femtosecond transient absorption spectra of **NI-PhMe$_2$-PTZ**. Transient absorption spectra (a) in HEX and (c) in ACN. Relative EADS obtained with global analysis (b) in HEX and (d) in ACN. Excited at 330 nm.

NI-PhMe$_2$-PTZ
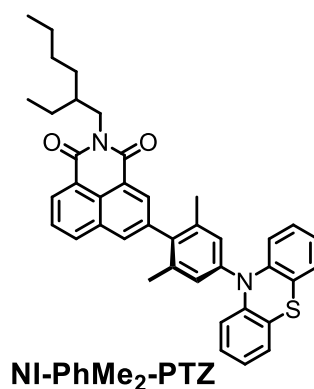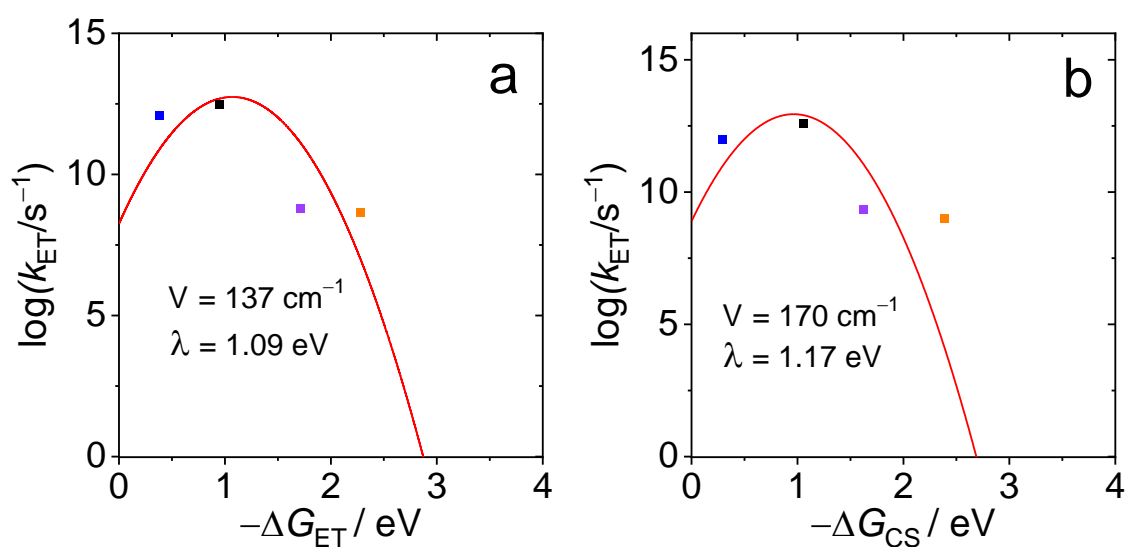
Figure S7. Plot of intramolecular electron-transfer rate constants in (a) **NI-PTZ** and (b) **NI-PTZ$_2$** *vs.* the thermodynamic driving force ($-\Delta G_{ET}$). The red line represents the best fit with Eq. 1. The data used are CS data (blue point) and CR data (orange point) in HEX, CS data (black point) and CR data (purple point) in ACN, respectively. The fitting program employs the nonlinear curve fitting toolkit from Origin 2019. The determination coefficient (R^2) is 0.36 of **NI-PTZ** and 0.34 of **NI-PTZ$_2$**. Due to the limited amount of data available, the goodness of fit is relatively low.

4. Time-resolved electron paramagnetic resonance spectroscopy
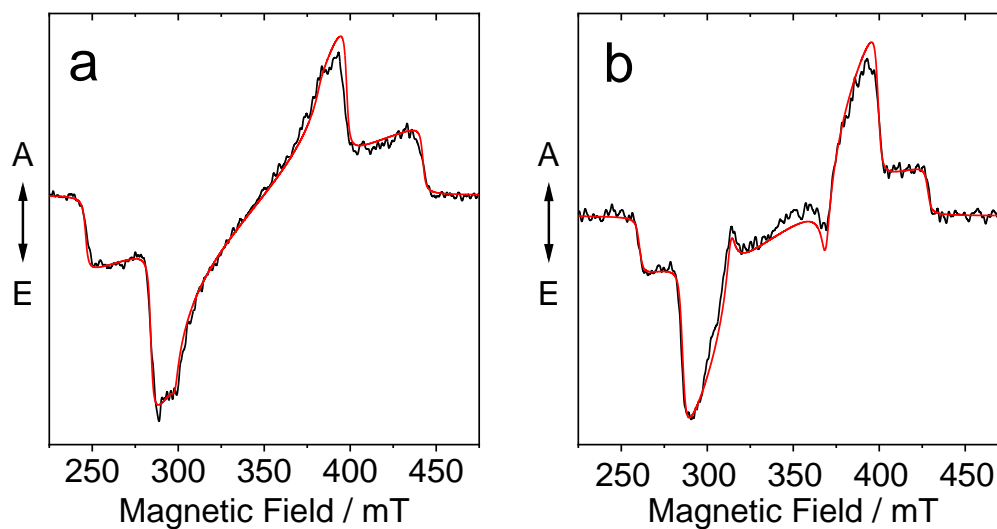
Figure S8. TREPR spectra of (a) **NI-3Br** and (b) **NI-Ph-Br**. The spectra were obtained under 355 nm laser, irradiation at 80 K in glassy toluene/2-methyltetrahydrofuran = 1:1 (v/v), c = 1×10^{-4} M, delay after flash (DAF) = 500 ns. Simulation spectra are shown in red, and experimental spectra are shown in black. Simulation parameters are presented in Table 2.
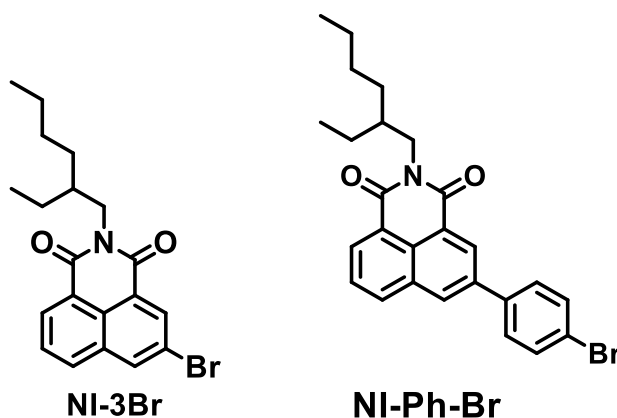
In order to further study the component in TREPR, two-pulse experiment at filed 350 mT were measured, shows the dependences of echo intensity vs. DAF at different temperatures and fitted by two exponentials with different lifetimes of ^{3}CS state (**Figure S9**). The different lifetimes of ^{3}CS state can attributed to $\tau(T_x)$ of 3 μs, while $\tau(T_z)$ of 30 μs. Taking these two lifetimes into account, the inversion of a narrow triplet spectrum (^{3}CS state) is quite well described (**Figure S10**) by the sum of two triplet spectra with different polarizations, and corresponding lifetimes.
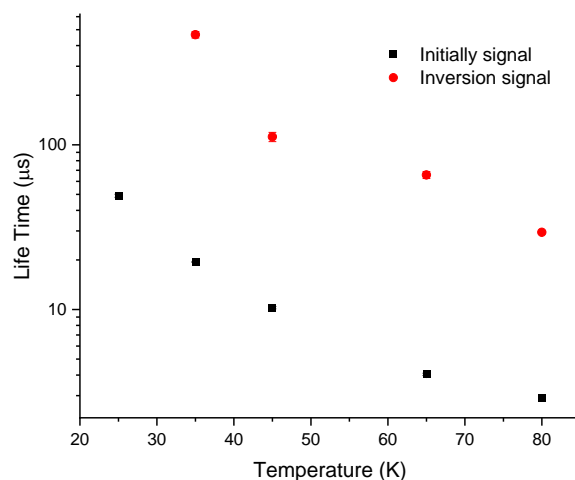
Figure S9. Temperature dependence of lifetimes of initially and inversion TREPR signals of Spectrum 1 in Figure 3b.
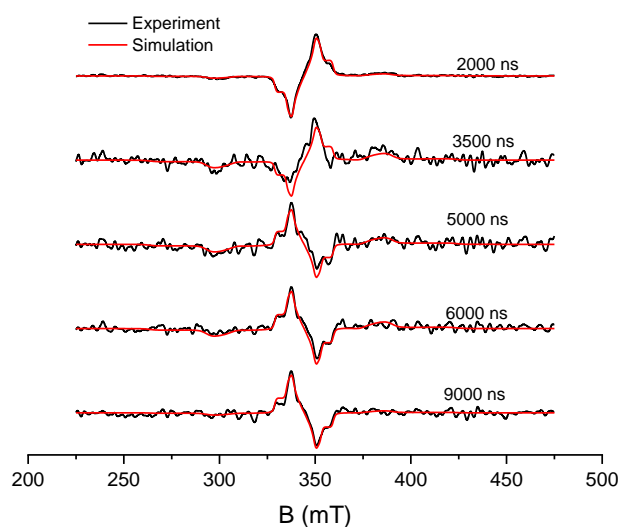
Figure S10. Experimental and simulated time dependence TREPR spectra of **NI-PTZ**. The spectra are simulated as the sum of three spectra: Spectrum 2 and Spectrum 1 (Figure 3b), Spectrum 1 is presented as the sum of two triplet spectra with lifetime τ = 30 μs and 3 μs, respectively. The agreement with experiment is quite good, but it is not realistic to assume that there are two triplets with the same fine structure parameters, but with different ESP patterns and lifetimes.
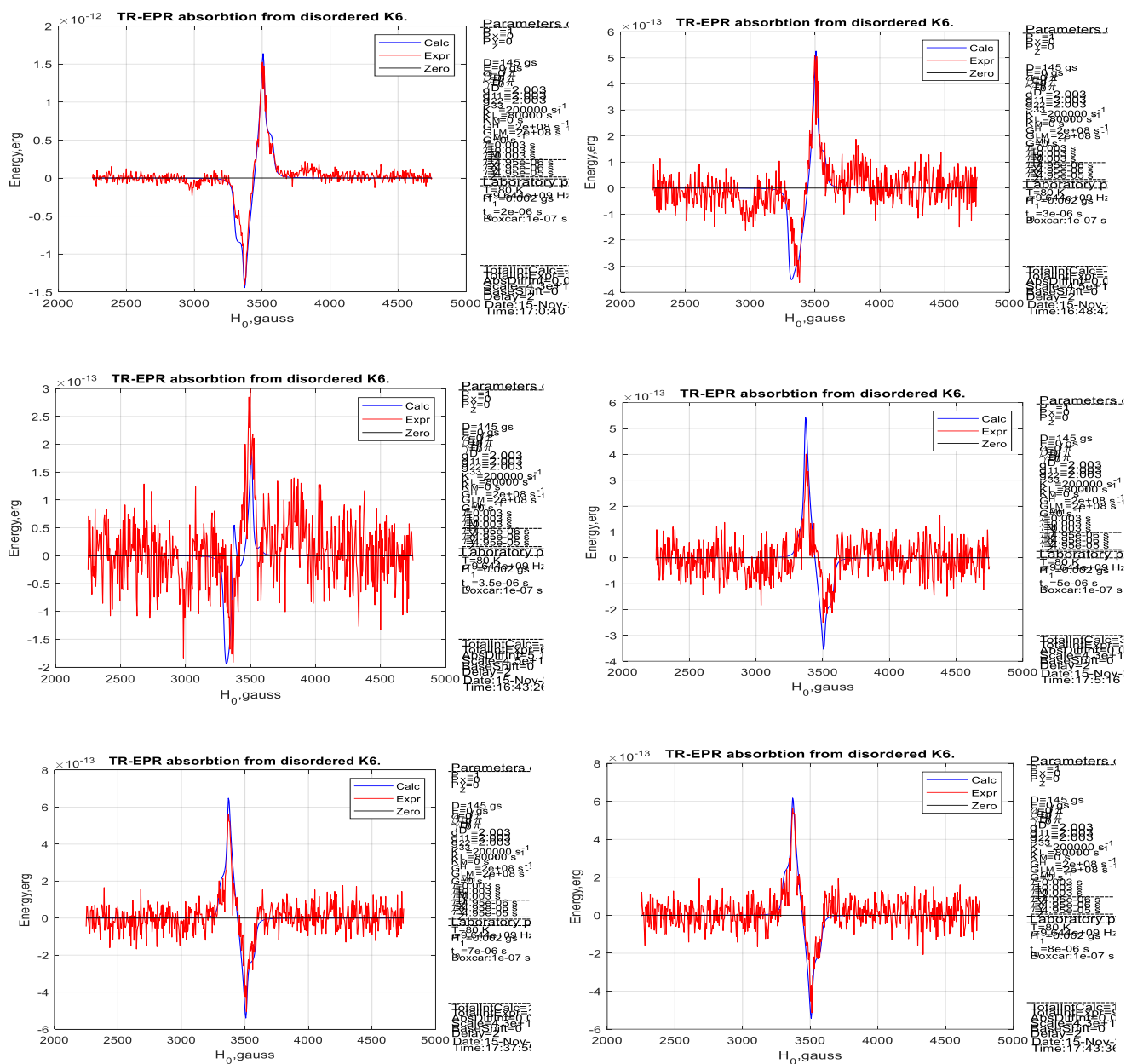
Figure S11. The time dependence of experimental (red) and simulated (blue, only ³CS sate)) TREPR spectra of **NI-PTZ** for DAF = 2000, 3000, 3500, 5000, 7000 and 8000 ns.
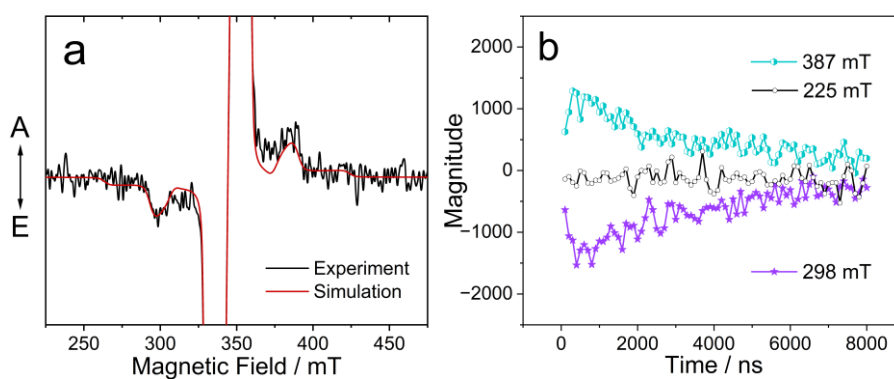
Figure S12. (a) The partially magnified spectrum in Fig. 3b. (b) Enhanced absorption/emission magnitude over delay time at 298 mT, 387 mT, and 225 mT (background noise).
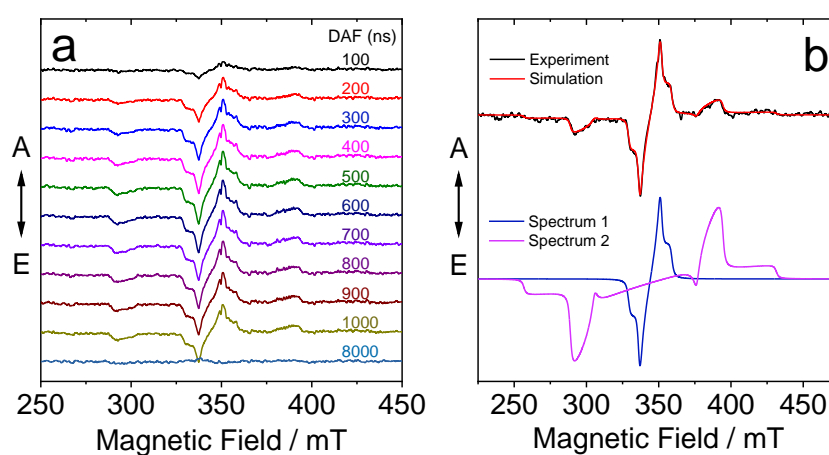
Figure S13. (a) Delay time-dependent evolution of the TREPR spectra and (b) the selected TREPR spectra of **NI-PTZ-O**. The spectra were obtained upon 355 nm pulsed laser, photoexcitation at 80 K in glassy toluene/2-methyltetrahydrofuran = 1:1 (v:v), c = 1×10^{-4} M, DAF = 500 ns. Simulation spectra are shown in red, and experimental spectra are shown in black. Simulation spectrum is sum of Spectrum 1 and Spectrum 2 with the weights 1 and 0.23, respectively. Simulation parameters are presented in Table 2. The inversion of the ESP phase pattern of spectrum 1 is observed at DAF ~8000 ns.
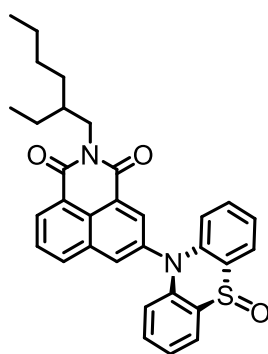
NI-PTZ-O
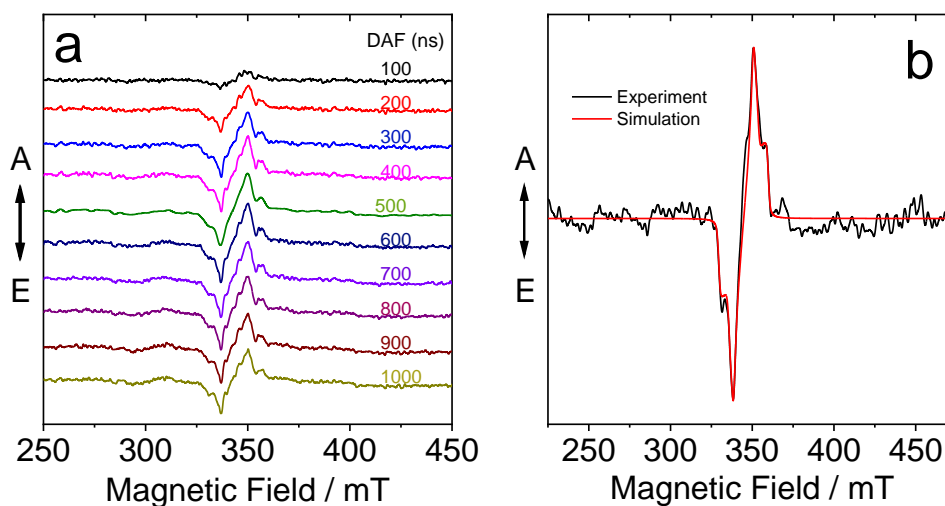
Figure S14. (a) Delay time-dependent evolution of the TREPR spectra and (b) the selected TREPR spectra of **NI-PTZ$_2$**. The spectra were obtained upon 355 nm pulsed laser, photoexcitation at 80 K in glassy toluene/2-methyltetrahydrofuran = 1:1 (v/v), c = 1×10^{-4} M, DAF = 500 ns. Simulation spectra are shown in red, and experimental spectra are shown in black. Simulation parameters are presented in Table 2.

NI-PTZ$_2$
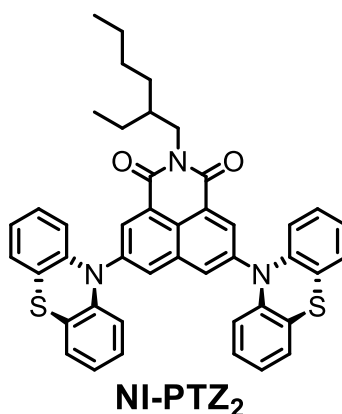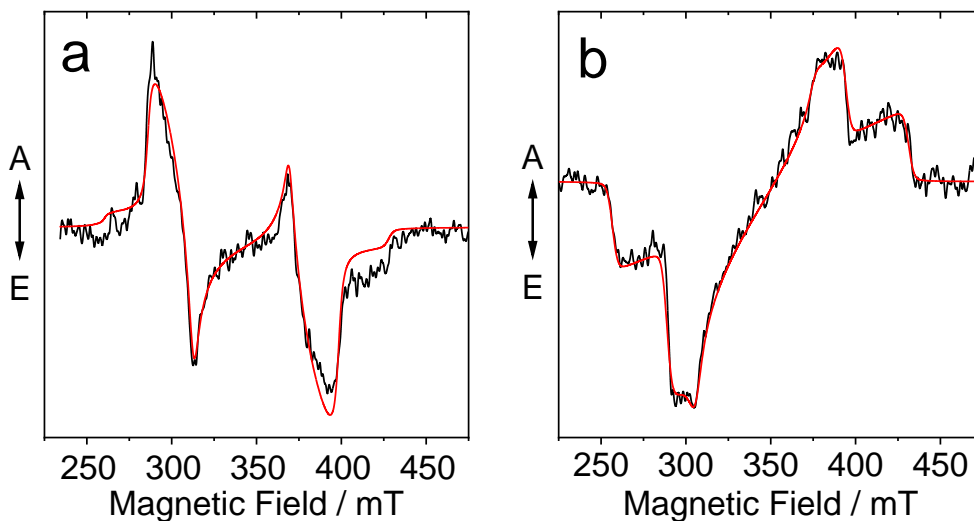
Figure S15. TREPR spectra of (a) **NI-Ph-PTZ** and (b) **NI-PhMe$_2$-PTZ**. The spectra were obtained upon 355 nm pulsed laser, photoexcitation at 80 K in glassy toluene/2-methyltetrahydrofuran = 1:1 (v/v), $c = 1\times10^{-4}$ M, DAF = 500 ns. Simulation spectra are shown in red, and experimental spectra are shown in black. Simulation parameters are presented in Table 2.

NI-Ph-PTZ

NI-PhMe$_2$-PTZ
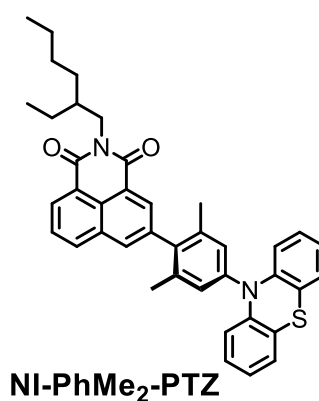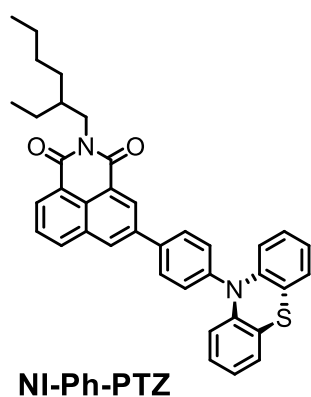
5. DFT calculations

Table S1. SOCME matrix elements constants incorporating the Herzberg-Teller terms.[a]

	T_{1y}-T_{2z}	T_{1y}-T_{2x}	T_{1z}-T_{2y}	T_{1z}-T_{2z}	T_{1x}-T_{2y}	T_{1x}-T_{2x}
gas-NI-PTZ	0.400544	0.400544	0.400544	0.619127	0.400544	0.619127
hex-NI-PTZ	0.400347	0.400347	0.400347	0.625721	0.400347	0.625721

[a] in cm^{-1}.

Table S2. The Zero-Field Splitting (ZFS) parameter D of **NI-PTZ**.[a]

T_1	T_2
0.05	0.01

[a] in cm^{-1}.

Reference

1 J. Snellenburg, S. Laptenok, R. Seger, K. Mullen, I. V. Stokkum, Glotaran: A Java-based graphical user interface for the R package TIMP, 2012, **49**.

2 Y. E. Kandrashkin, M. S. Asano, A. van der Est, *J. Phys. Chem. A*, 2006, **110**, 9607–9616.

3 Y. E. Kandrashkin, M. S. Asano, A. van der Est, *J. Phys. Chem. A*, 2006, **110**, 9617–9626.

4 G. W. T. M. J. Frisch, H. B. Schlegel, G. E. Scuseria, M. A. Robb, J. R. Cheeseman, G. Scalmani, V. Barone, B. Mennucci, G. A. Petersson, et al., Gaussian 16 Rev., Wallingford, CT, 2016.

5 Y. Shao, Z. Gan, E. Epifanovsky, A. T. Gilbert, M. Wormit, J. Kussmann, A. W. Lange, A. Behn, J. Deng, X. Feng, et al., *Mol. Phys.*, 2015, **113**, 184–215.

6 S. Hirata, M. Head-Gordon, *Chem. Phys. Lett.*, 1999, **314**, 291–299.

7 F. Wang, T. Ziegler, *J. Chem. Phys.*, 2005, **123,** 154102.